BNL-41667
CONF-880335--23

SPACE CHARGE EFFECT AT TRANSITION ENERGY AND THE TRANSFER OF R.F. SYSTEM AT TOP ENERGY

J. Wei and S.Y. Lee

Accelerator Development Department
Brookhaven National Laboratory
Upton, New York 11973

BNL--41667
DE88 016584

Abstract

Using 100 kV R.F. system, the beam loss due to transition crossing can be reduced to 1% for the phase space area of $0.3ev \cdot sec/amu$. However the space charge effect would increase the phase space area to $1ev \cdot sec/amu$ after the transition energy. By using $\dot{\gamma}_t$ jump or $\dot{\gamma}$ increase, the phase space area can be preserved to $0.3ev \cdot sec/amu$. To obtain small bunch length at the collision energy, we study the bunch rotation scheme. We find that the R.F. harmonic number should be less than 6×342 to obtain good efficiency and larger than 4×342 to reach experimental requirement.

* Research has been carried out under the U.S.D.O.E.

I. INTRODUCTION

The R.F. system originally proposed for the Relativistic Heavy Ion Collider is operated at R.F. frequence $26.74MHz$ and peak voltage $1.2MV$, which was dictated by the need to provide sufficient longitudinal phase space area to accommodate the bunch area dilution due to intrabeam scattering in the beam storage mode. During the acceleration period the stable phase angle is $\sin\phi_s = 0.04$.

The longitudinal phase space area at injection is taken to be $0.3ev \cdot sec/amu$ for heavy ions. Around the transition region , the beam momentum spread is about $\pm 0.5\%$. The time when the kinematic non-linear effect becomes important is much longer than the non-adiabatic γ_t crossing time [1,2], as listed in Table 1. Thus the kinematic non-linear effect dominates the entire transition region. Fig. 1 shows the γ_t crossing of $^{197}Au^{+79}$ ions. Even without considering the space charge effect, there is a 70% beam loss. Therefore method of γ_t jump or $\dot{\gamma}$ increasing is needed to achieve a high transition energy crossing efficiency.

According to the new R.F. scenario raised on this workshop, the R.F. parameters are changed to $\hat{V} = 100kV$ and $\sin\phi_s = 0.48$ to maintain the same acceleration rate. For gold ions, the bucket area is $0.6\ ev \cdot sec/amu$ at the injection energy of $\gamma = 13$. The beam momentum spread is 1.8 times smaller than that in the original $1.2MV$ peak voltage scenario, while the non-adiabatic γ_t crossing time is more than two times longer. The beam passes through the transition energy with a much higher efficiency.

In Section II we shall present the result of γ_t crossing under the new R.F. scenario. First we review briefly the equations of motion for the longitudinal space in the transition energy region in Section IIa. The beam induced space charge effect is discussed in Section IIb. In Section IIc we shall describ the treatment of using γ_t jump or $\dot{\gamma}$ increase.

It is suggested on the workshop that method of bunch rotation at top energy should be used to achieve shorter bunches for experimental use. In Section III we shall explore various bunch rotation scenarios using different R.F. rotation voltage and different high

frequency R.F. system. The result is compared in Section IV with the scheme of using high frequency R.F. system by the time the beam crosses the transition energy, as proposed by *M. Brennan* [3] on this workshop.

II. $\hat{V} = 100kV$, $\sin\phi_s$ =0.48 R.F. SYSTEM ON γ_t CROSSING

A. Tracking Simulation and Kinematic Mismatching Effect

The evolution of $^{197}Au^{+79}$ ions in the longitudinal phase space is shown in Fig. 2. Below transition energy the bunch is assumed to have a bi-gaussian distribution of phase space area 0.3 $ev \cdot sec/amu$. The motion of each individual particle in the longitudinal phase space $(\phi, \frac{\Delta E}{\Omega_0})$ is described by the difference equations

$$\begin{aligned}\delta_{n+1} &= \delta_n + \frac{Ze\hat{V}_{1,n}}{Am_0c^2\gamma_{s,n}} \cdot (\sin\phi_n - \sin\phi_{s,n}) \\ &\quad + \frac{Ze\hat{V}_{2,n}}{Am_0c^2\gamma_{s,n}} \cdot (\sin(\phi_{2,s,n} + \frac{h_2}{h_1}\Delta\phi_n) - \sin\phi_{2,s,n}) \\ &\quad + \Delta_{s.c}(\phi_n) + \Delta_Z(\phi_n) \qquad (1)\end{aligned}$$

$$\phi_{n+1} = \phi_n + \frac{2\pi h\eta_n(\delta_{n+1})}{\beta^2_{s,n}} \cdot \delta_{n+1} \qquad (2)$$

where

$\gamma_s = (1-\beta_s^2)^{-\frac{1}{2}}$, synchronous energy of the particle in m_0c^2 units

h_1 = harmonic number of the original acceleration R.F. system

h_2 = harmonic number of the high frequency R.F. system used for bunch rotation or γ_t crossing programming

$\delta = \frac{\Delta E}{E_s} = \frac{\Delta\gamma}{\gamma_s} = \beta_s^2\frac{\Delta p}{p_s}$, relative deviation of the particle energy

ϕ = deviation of the particle R.F. phase from ϕ_s in the original R.F. phase space

Z = charge carried by the particle

A = atomic number of the particle

$\Delta_{s.c.}$ = relative energy gain per turn due to the space charge field

Δ_Z = relative energy gain per turn due to coupling impedance

n (subscript) = revolution number.

The kinematic non-linearity is included in equation (1,2) ,

$$\eta_n(\delta) = \eta_0(\gamma_{s,n}) + \eta_1(\gamma_{s,n})\frac{\Delta p}{p} + \dots \tag{3}$$

where

$$\eta_0(\gamma_{s,n}) = \frac{1}{\gamma_{t0}^2} - \frac{1}{\gamma_{s,n}^2} \ , \ \eta_1(\gamma_{s,n}) = \frac{3\beta_{s,n}^2}{2\gamma_{s,n}^2} - \frac{\alpha_1}{2\gamma_{t0}^2} \ , \tag{4}$$

with α_1 as the expansion coefficient of the momentum compaction factor α, *i.e.*

$$\alpha = \alpha_0(1 + \alpha_1\frac{\Delta p}{p} + \dots) \ ; \ \alpha_0 = \frac{1}{\gamma_{t0}^2} \ , \tag{5}$$

where γ_{t0} is the transition energy of the machine. The particles are tracked further on a turn-by-turn basis to higher energy

$$\gamma_{s,n+1} = \gamma_{s,n} + \frac{Ze\hat{V}_{1,n}}{Am_0c^2}\sin\phi_{s,n} + \frac{Ze\hat{V}_{2,n}}{Am_0c^2}\sin\phi_{2,s,n} \ . \tag{6}$$

If the line density $\lambda(\phi)$ of the beam changes slowly [4,5] within distance comparable to the diameter of the vacuum chamber 2b ,*i.e.*

$$\frac{2b}{\lambda}\frac{\partial\lambda}{\partial s} \ll 1 \ , \tag{7}$$

the space charge induced voltage effect, $\Delta_{s.c.}(\phi_n)$, can be represented by the mean field expression

$$\Delta_{s.c.}(\phi_n) = \frac{eV_{s.c.}(\phi_n)}{Am_0c^2\gamma_s} = \frac{Z_0g_0R_0cZe}{2Am_0c^2\gamma_s^3}\cdot\frac{\partial\lambda(\phi_n)}{\partial s} \ , \tag{8}$$

where $Z_0 = (\varepsilon_0 c)^{-1} = 377\ (\Omega)$, R_0 is the average radius of curvature. g_0 is the geometric factor, $g_0 = 1 + 2\ln\frac{b}{a}$ for a cylindrical geometry.

The voltage induced by the space charge $V_{s.c.}(\phi)$ is found by evaluating the derivative of the density distribution function of the beam in the ϕ space [4,5]

$$V_{s.c.}(\phi) = \frac{Z^2h^2g_0Z_0ce}{2R_0\gamma_s^2}\cdot\frac{\partial(N_0f(\phi))}{\partial\phi} \ , \tag{9}$$

where N_0 is the total number of particles per bunch, $N_0f(\phi)$ is the number of particles per unit ϕ around ϕ_s. To study the effect of microwave instability, the bin length used in the calculation should be of the order of the wave length of microwave cutoff, *i.e.*, $l_b \sim b$.

The time scales relevant to the problem are the following:

1. τ_0, revolution period;
2. $\tau_{sym.}$, synchrotron oscillation period;
3. $T_{n.l.}$, nonlinear time, during which the η_1 contributes more than η_0,

$$T_{n.l.} = \frac{\Delta\gamma}{\dot{\gamma}} = \frac{(3\beta_s^2 - \alpha_1)\cdot(\frac{\Delta p}{p})_{2.5\sigma}}{4\dot{\gamma}} \quad (10)$$

where $(\frac{\Delta p}{p})_{2.5\sigma}$ is the half total momentum spread of the beam;

4. T_c, characteristic nonadiabatic time[1]

$$T_c = \left(\frac{Am_0c^4}{R_0^2 h}\cdot\frac{\gamma_t^4}{2\dot{\gamma}}\cdot\frac{2\pi}{ZeV|\cos\phi_s|}\right)^{\frac{1}{3}}, \text{and}$$

5. $T_{m.w.}$, microwave instability growth time[1]. (11)

With the new R.F. system, the total momentum spread of the beam is about $\frac{\Delta p}{p} = \pm 0.25\%$ by the time the bunch is near the transition energy. Comparing with the original scenario, the non-linear time now becomes shorter than the characteristic time (see Table 1),

$$\tau_0 \ll T_{n.l.} < T_c < \tau_{sym.} . \quad (12)$$

From Fig. 2 we observe that few particles are spilled out of the bucket due to the kinematic effect. Without considering the space charge contribution, 99% of the particles remain inside the bucket after they cross the transition energy. The central "core" consists of about 95% beam. It has roughly the same 95% phase space area as before the γ_t crossing. The "tail" beam will gradually wind up around the central "core" beam.

B. Effects of Beam Induced Space Charge

During the computer simulation 3600 representative particles are used for the study of the beam induced space charge effect. The bin size used in the calculation is chosen to be the vacuum pipe aperture of 0.072 m. Therefore space charge voltage contribution from low frequency to microwave cutoff is included in the calculation. With an intensity of 1.1×10^9 per bunch, the space charge gives an equivalent capacitive impedance of

$\frac{Z}{n} \sim 1.2\ \Omega$ at transition energy. Contributions from the space charge and the kinematic non-linearity are both included. The phase space diagrams corresponding to Fig.2 are shown in Fig.3.

We observe that although the instability is expected to happen during the time $T_{m.w.}$ after the beam crosses the transition energy[1], the effect from the low frequency defocusing space charge force combined with the kinematic non-linearity is dominant. From Fig.3c and the corresponding space charge voltage curve Fig.4c we notice that the negative space charge voltage on the positive $\Delta\phi$ side drives the two "tails", one developed before and the other after the central γ_{t0} crossing as shown in Fig.2c, far away from the center. Although the γ_t crossing efficiency is still 98% , the phase space area is blown up. From Fig.3d we see strong diffusion and filamentation in the longitudinal space. The macroscopic phase space area after γ_t crossing is about $1ev \cdot sec/amu$.

To investigate the effect of space charge and impedance induced field, we perform the calculation under several circumstances, as shown in Table 2. Fig.5 corresponds to the case when the kinematic non-linearity is neglected, $\alpha_1 = 0$, and when the space charge capacitive impedance $\frac{Z}{n} \sim 1.2\ \Omega$. We observe that the space charge force causes bunch length mismatching. After the transition crossing the bunch tumbles in the longitudinal space. The phase space area increases to about $0.6ev \cdot sec/amu$.

Fig.6 shows the case where there is an inductive impedance $|\frac{Z}{n}| \sim 1.2\ \Omega$ by the time the beam crosses the transition energy. At the moment before the central γ_{t0} crossing the space charge voltage enhances the developing of the non-linear "tail", as shown in Fig.6b. The crossing efficiency is 97%. The phase space area after γ_t crossing is about $1ev \cdot sec/amu$. The transition energy crossing behaviour is very similar to that of the capacitive impedance case (Fig.3).

Fig.7 corresponds to the situation when the impedance is strong, a capacitive $\frac{Z}{n} \sim 10\ \Omega$. We observe that during the time $T_{m.w.}$ after the central γ_{t0} crossing the instability develops. The original bunch breaks into many short bunches, as shown in Fig.7b. The instability and the kinematic non-linearity causes strong beam loss. After the beam is

far away beyond the γ_t, the synchrotron oscillation motion diffuses the distribution, as shown in Fig.7*d*. The crossing efficiency is 79%. Due to filamentation the beam will gradually fill up the entire bucket.

C. γ_t Jump Crossing Transition Energy

We assume that the quadrupoles are pulsed in a way that γ_t is jumped by $\Delta\gamma = 0.6$ within $60ms$ by the time the beam crosses γ_{t0}. Effectively the beam passes the transition energy region with an effective $\dot{\gamma}$ faster by a factor of 6. As shown in Table 1, in this case

$$\tau_0 \ll T_{n.l.} \ll T_c < \tau_{syn.} . \tag{13}$$

The kinematic non-linear effect and the space charge effect are both cured by such a fast γ_t crossing. The simulation of the γ_t jump process is shown in Fig.8. No beam loss and essentially no phase space area blow up is observed. Instead of γ_t jump, a $\dot{\gamma}$ increase by using the available momentum aperture can similarly improve the crossing efficiency.

III. BUNCH ROTATION SCENARIO & REQUIREMENTS

A. Bunch Rotation at Collision Energy

The bunched beam of particles is accelerated by the R.F. system of peak voltage of $\hat{V}_1 = 100kV$, harmonic number of $h = 342$ to the top collision energy. The method of bunch rotation can be applied to squeeze and rotate the bunch to a shorter bunch length. A high frequency R.F. system is snapped on at this moment to recapture the bunch in the new R.F. bucket. The beam thus has a much shorter bunch length for experimental use.

The R.F. voltage is adiabatically decreased from $\hat{V}_1 = 100kV$ to a lower voltage $\hat{V}_2$. From Fig.9*b* we notice that $\hat{V}_2 = 50kV$ provides enough phase space area for the $1ev \cdot sec/amu$ beam. The bunch is vertically compressed to have a smaller momentum spread ($\frac{\Delta p}{p}$) and a longer bunch length $\Delta\phi$. A voltage $\hat{V}_3$ of the same R.F. frequency

is applied to rotate the bunch for a time period of about $\frac{1}{4}$ synchrotron oscillation. As shown in Fig.9c, the bunch length becomes very short. The other R.F. system with new harmonic number h_2, peak voltage $\hat{V}_4$ is snapped on at this time.

Hence, the requirements for the bunch rotation are:

1. $\hat{V}_2$ should not be too small, *i.e.* the bunch should not be squeezed too much. Otherwise the "tail" particles suffer too much from the non-linear R.F. rotation;

2. the bunch length after the rotation of $\frac{1}{4}$ synchrotron oscillation period under voltage $\hat{V}_3$ should be short enough for the high frequency R.F. bucket, *i.e.*

$$\Delta\phi_3 < \frac{2\pi h_1}{h_2} ; \tag{14}$$

3. the minimum voltage $\hat{V}_3$ for the bunch rotation is decided by the momentum spread after the compression $(\frac{\Delta p}{p})_2$ and the required bunch length $\Delta\phi_3$,

$$\hat{V}_{3,min.} = \frac{2\pi\gamma_s h_1 |\eta_s| \beta_s^2 A m_0 c^2}{Z|\cos\phi_s|} \cdot \left(\frac{(\frac{\Delta p}{p})_2}{\Delta\phi_3}\right)^2 . \tag{15}$$

A higher $\hat{V}_3$ gives a more linear rotation and thus improves the efficiency;

4. the high frequency R.F. system with harmonic number h_2 should have a peak voltage

$$\hat{V}_4 \sim \frac{h_2}{h_1} \cdot \hat{V}_3 . \tag{16}$$

The voltage $\hat{V}_3$, $\hat{V}_4$ and the synchrotron oscillation frequency Ω_s depend on the required top energy γ_{top}. For a specific h_2, both $\hat{V}_3$ and Ω_s are proportional to the quantity $\sqrt{\frac{|\eta_{top}|}{\gamma_{top}}}$. In Fig.10 the quantity $\sqrt{\frac{|\eta_{top}|}{\gamma_{top}}}$ is plotted as a function of the top energy γ_{top}. Fig.10 implies that between γ_{top} =30 and γ_{top} =100 the bunch rotation scenario is appliable.

B. Results For $^{197}Au^{+79}$ Ions

Bunch rotation simulation is done for the $^{197}Au^{+79}$ ions with various beam populated phase space area, rotation voltage $\hat{V}_3$ and harmonic number h_2. In the simulation for

the beam of phase space area of $1ev \cdot sec/amu$ and $0.5ev \cdot sec/amu$, the voltage is first decreased from $\hat{V}_1$ =100kV to $\hat{V}_1 = 50kV$ in $50ms$ and from $\hat{V}_1$ =100kV to $\hat{V}_2 = 15kV$ in $100ms$ respectively. Then the R.F. voltage is increased to $\hat{V}_3$ in half milli-second. Two schemes are investigated, $\hat{V}_3 = 300kV$ and $\hat{V}_3 = 500kV$. The voltage is kept at $\hat{V}_3$ for $12ms$ and $8ms$ respectively. After this time period the high frequency R.F. system with $\hat{V}_4$, h_2 is snapped on in half milli-second. By the same time the $h_1 = 342$ R.F. system is turned off. This procedure can be applied for various collision energy from γ_{top} =30 to γ_{top} =100.

Fig.11 shows the longitudinal phase space diagrams after the recapture for $\hat{V}_3$ =500kV and h_2 =1710, 2052 and 2736 respectively at γ_{top} =30. The R.F. voltage is $\hat{V}_4 = 2.5MV$, $3MV$ and $4MV$ respectively. The beam populated phase space area is assumed to be $1ev \cdot sec/amu$ before the bunch rotation, as shown in Fig.9a.

Fig.12 shows the total efficiency of the bunch rotation process for γ_{top} =30. The $\hat{V}_3$ =500kV scheme improves upon the $\hat{V}_3$ =300kV one by reducing the bunch length $\Delta\phi_3$ and by reducing the non-linear R.F. rotation. In either scheme, the bunch of $1ev \cdot sec/amu$ is too wide for the h_2 =2736 bucket. Either the beam phase space area should be reduced or the h_2 be decreased to achieve a bunch rotation efficiency above 95%. At γ_{top} =30 the effect due to the beam induced space charge field is within 1%. The result for γ_{top} =100 is the same as the one for γ_{top} =30, as shown in Fig.12, except that the space charge effect is negligible.

In Fig.13 we plot the achievable *R.M.S.* bunch length σ_l as a function of the harmonic number h_2 for the phase space area before the rotation, $1ev \cdot sec/amu$ and $0.5ev \cdot sec/amu$ respectively. The R.F. peak voltage is assume to be $1.2MV$ for $h_2 = 342$ and $15MV$ for $h_2 = 8 \times 342$. The larger the h_2, the higher the voltage. For the top energy phase space area of $1ev \cdot sec/amu$, the experimental requirement of $\sigma_l \sim 0.2$ m implies that h_2 should be larger than 4×342. However to achieve a rotation efficiency of above 95%, h_2 should not be larger than 6×342. The requirement on short bunch length compromises with the rotation efficiency to a range of h_2 from 4×342 to 6×342. If γ_t jump or other methods

are employed to ensure that the top energy phase space area is within $0.5ev \cdot sec/amu$, this range can be extended to from 3×342 to 8×342.

IV. COMPARISON WITH SCENARIO OF TRANSFERING TO HIGH FREQUENCY R.F. SYSTEM DURING γ_t CROSSING

We shall compare the scenario described in Section II and III with the one of transfering to the high frequency R.F. system during the transition energy crossing time, as being discussed in Ref.3. Because the bunched beam has a relatively short bunch length by the time it crosses the transition energy, it is possible to program the R.F. systems such that the beam is recaptured in the high frequency R.F. bucket after it crosses the transition energy. Thereafter the beam is accelerated to the collision energy by the high frequency R.F. system.

Simulation is done[3] by adiabatically turn on the high frequency R.F. system with harmonic number h_2. The peak voltage of this system is gradually increased from 0 to $\frac{h_2}{h_1} \times 100(kV)$ in about $1sec.$ after the center of the bunch crosses γ_{t0}. The phase space area below transition energy is assumed to be $0.3ev \cdot sec/amu$. A non-linear $\alpha_1 = -0.6$ is again assumed. In Fig.14 the efficiency is plotted as a function of h_2. Note that the bucket provided by the h_2 =2736 R.F. system is too narrow for the beam phase space area of $0.3ev \cdot sec/amu$.

Acknowledgment

We would like to thank Dr. *E.D. Courant* for many enlightening discussions on the kinematic non-linear effect during γ_t crossing. We would also like to thank all the people in the R.F. group of this workshop for many stimulating discussions on the new R.F. scenario. We thank Dr. *A.G. Ruggiero* and Dr. *J. Claus* very much for the very helpful discussions on the space charge effect calculation.

TABLES

Table 1. – Characteristic non-adiabatic γ_t crossing time T_c and non-linear time $T_{n.l.}$

	T_c (ms)	$T_{n.l.}$ (ms)	95% phase space area $(ev \cdot sec/amu)$	Survival rate
Original $\hat{V} = 1.2MV, \sin\phi_s = 0.04$ scenario	26	63		30%[a] (Fig.1)
$\hat{V} = 1.2MV, \sin\phi_s = 0.04$ with γ_t jump $\Delta\gamma_t = 0.6$ in $30ms$	11	5	0.3[a]	100%[a]
New $\hat{V} = 100kV, \sin\phi_s = 0.48$ scenario	57	36	0.3[a]	99.1%[a] (Fig.2)
			1.[b]	97.9%[b] (Fig.3)
$\hat{V} = 100kV, \sin\phi_s = 0.48$ with γ_t jump $\Delta\gamma_t$=0.6 in $60ms$	31	6	0.3[a]	100%[a]
			0.3[b]	100%[b] (Fig.8)

Calculation is performed for $^{197}Au^{+79}$ ions of 1.1×10^9 per bunch. $\gamma_{t0} = 25.44$. The initial phase space area is assumed to be $0.3ev \cdot sec/amu$.

a) Calculation is done without considering the space charge induced fields.

b) Space chsrge effect is included in the calculation. The bin size is chosen to be the vacuum pipe aperture of $0.072m$. $\frac{Z}{n} \sim 1.2\ \Omega$. Calculation is done with 3600 representative particles and by using the three-point formula[4].

Table 2. – Space charge and impedance induced effect

	95% phase space area ($ev \cdot sec/amu$)	survival rate	Features
No space charge no impedance $\alpha_1 = -0.6$	0.3	99%	Non-linear "tail" and filamentation (Fig.2)
Space charge $\frac{Z}{n} = 1.2\Omega$ $\alpha_1 = 0$	0.6	100%	bunch length mismatching and tumbling (Fig.5)
Space charge $\frac{Z}{n} = 1.2\Omega$ $\alpha_1 = -0.6$	1	98%	non-linear "tail" tumbling and diffusion (Fig.3)
Inductive $\left\|\frac{Z}{n}\right\| = 1.2\Omega$ $\alpha_1 = -0.6$	1	97%	non-linear "tail" tumbling and diffusion (Fig.6)
Capacitive $\frac{Z}{n} = 10\Omega$ $\alpha_1 = -0.6$	1~2	79%	microwave instability and diffusion (Fig.7)
γ_t jump $\Delta\gamma_t$=0.6 in $60ms$ space charge $\frac{Z}{n} = 1.2\Omega$ $\alpha_1 = -0.6$	0.3	100%	"clean" crossing (Fig.8)

$\hat{V} = 100kV$, $\sin\phi_s = 0.48$ R.F. system for $^{197}Au^{+79}$ ions of 1.1×10^9 per bunch. $\gamma_{t0} = 25.44$. The initial phase space area is assumed to be $0.3ev \cdot sec/amu$. For the space charge and impedance calculation, the bin size is chosen to be the vacuum pipe aperture of $0.072m$. $\frac{Z}{n} \sim 1.2\ \Omega$. Calculation is performed with 3600 representative particles and by using the three-point formula[4].

REFERENCES

1) S.Y. Lee and J.M. Wang, IEEE vol. NS-52, pp 2323(1985)

2) *Conceptual Design of the RHIC*, May (1986)

3) M. Brennan *et. al.*, this proceeding

4) J. Wei, S.Y. Lee and A.G. Ruggerio, Booster Tech. Notes, No. 115(1988)

5) W.W. Lee and L.C. Teng, CERN Conference, pp328(1971)

FIGURE CAPTIONS

Fig. 1. The transition energy crossing with the $\hat{V}$ =1.2MV, h =342 R.F. system. $\sin\phi_s$ =0.04. Space charge effect is not considered. Efficiency is 30%.

Fig. 2. The transition energy crossing with the $\hat{V}$ =100kV, h =342 R.F. system. $\sin\phi_s$ =0.48. Space charge effect is not considered. Efficiency is 99.1%.

Fig. 3. The transition energy crossing with the $\hat{V}$ =100kV, h =342 R.F. system. $\sin\phi_s$ =0.48. Space charge effect is considered. The space charge impedance $\frac{Z}{n} = 1.2\Omega$. Efficiency is 97.9%. The phase space area is estimated to be $1ev \cdot sec/amu$ after the γ_t crossing.

Fig. 4. The space charge voltage curve corresponding to Fig.3. The maximum vertical scale corresponds to the acceleration voltage of $\hat{V} \cdot \sin\phi_s$.

Fig. 5. The transition energy crossing with the $\hat{V}$ =100kV, h =342 R.F. system. $\sin\phi_s$ =0.48. Only the space charge effect is considered. The space charge impedance $\frac{Z}{n} = 1.2\Omega$. Efficiency is 100%. The phase space area is estimated to be $0.6ev \cdot sec/amu$ after the γ_t crossing.

Fig. 6. The transition energy crossing with the $\hat{V}$ =100kV, h =342 R.F. system. $\sin\phi_s$ =0.48. A total inductive impedance of $|\frac{Z}{n}| = 1.2\Omega$ is assumed. Efficiency is 96.8%. The phase space area is estimated to be $1ev \cdot sec/amu$ after the γ_t crossing.

Fig. 7. The transition energy crossing with the $\hat{V}$ =100kV, h =342 R.F. system. $\sin\phi_s$ =0.48. A total capacitive impedance of $\frac{Z}{n} = 10\Omega$ is assumed. Efficiency is 79.2%. The phase space area is estimated to be 1~2 $ev \cdot sec/amu$ after the γ_t crossing.

Fig. 8. The transition energy crossing with the $\hat{V}$ =100kV, h =342 R.F. system. $\sin\phi_s$ =0.48. The machine γ_{t0} is jumped by $\Delta\gamma_t$ =0.6 in 60ms. Space charge effect is considered. The space charge impedance $\frac{Z}{n} = 1.2\Omega$. Efficiency is 100%. No phase space area blow up is observed.

Fig. 9. Bunch rotation at top energy γ_{top} =30 . The phase space area is $1ev \cdot sec/amu$. $\hat{V}_1$ =100kV, $\hat{V}_2$ =50kV and $\hat{V}_3$ =500kV. The harmonic number is h_1 =342.

Fig. 10. $\sqrt{\frac{|\eta|}{\gamma}}$ as a function of γ_{top}

Fig. 11. Bunch rotation recapture at top energy of γ_{top} =30 . The space charge effect is considered. h_2 =1710, 2052 and 2736 respectively. The phase space area is $1ev \cdot sec/amu$. $\hat{V}_1$ =100kV, $\hat{V}_2$ =50kV, $\hat{V}_3$ =500kV, h_1 =342.

Fig. 12. Bunch rotation efficiency at top energy of γ_{top} =30 under variour $\hat{V}_3$, h_2 and phase space area.

Fig. 13. *R.M.S.* bunch length σ_l as a function of h_2 for different top energy phase space area.

Fig. 14. Efficiency of the scheme of transfering to the high frequency R.F. system during the γ_t crossing. h_2 =1710, 2052 and 2736 respectively. The phase space area below transition energy is $0.3ev \cdot sec/amu$. Space charge effect is not considered.

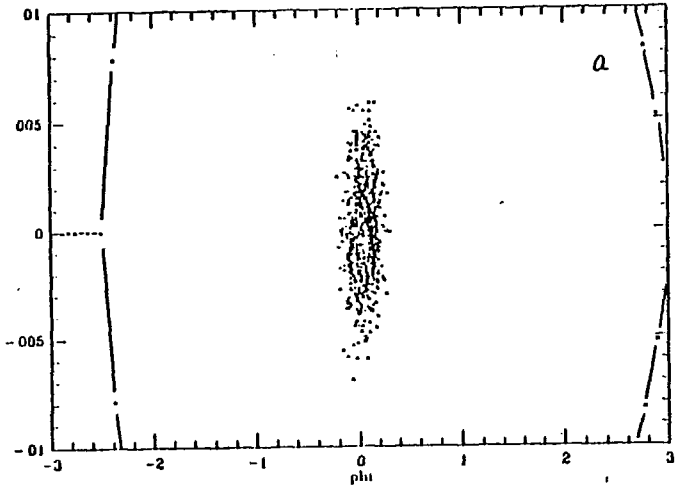

- 80 ms

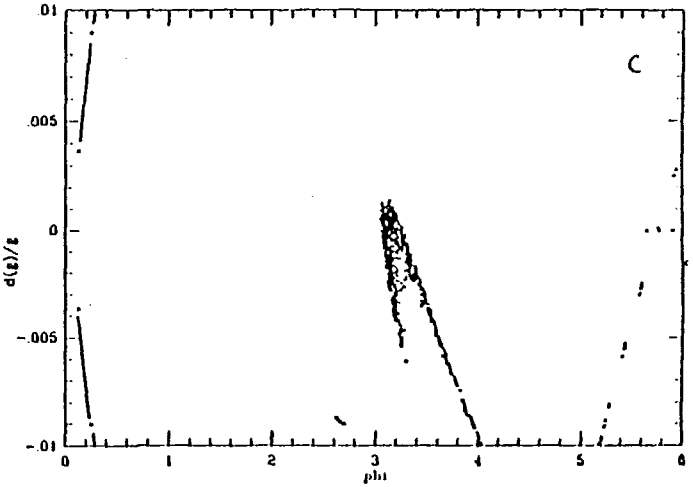

+ 25 ms

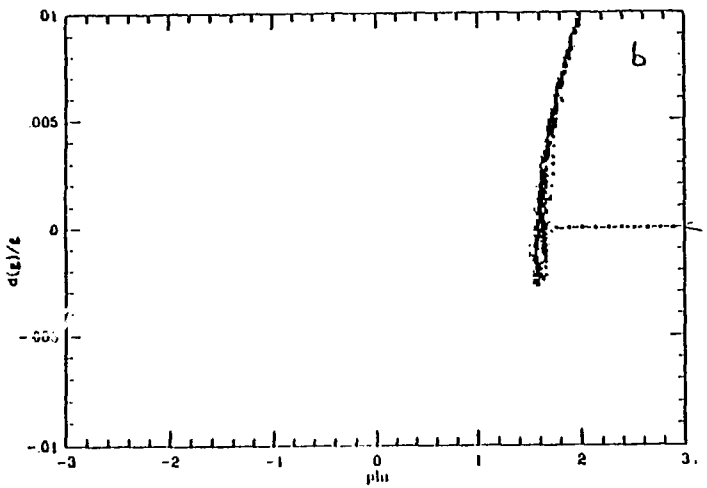

0 ms

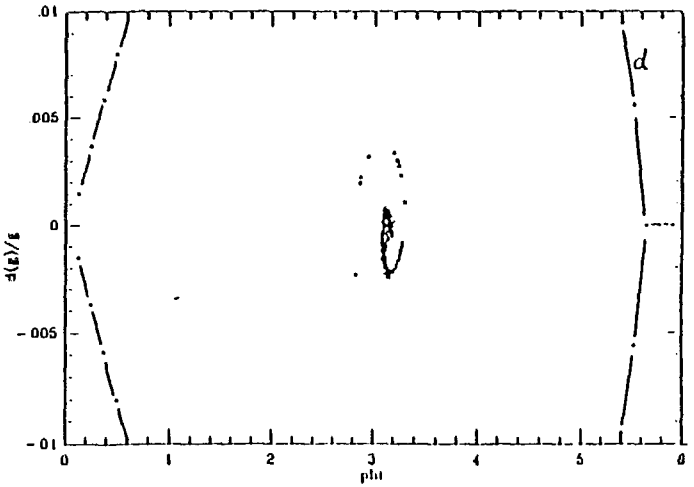

+ 180 ms

Fig. 1

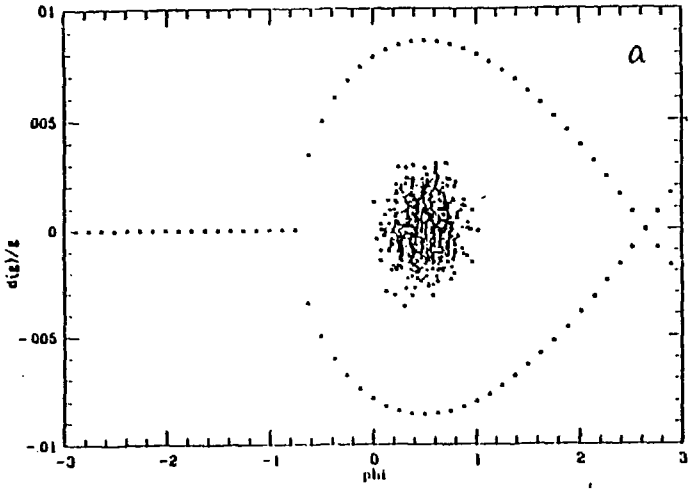

-80 ms

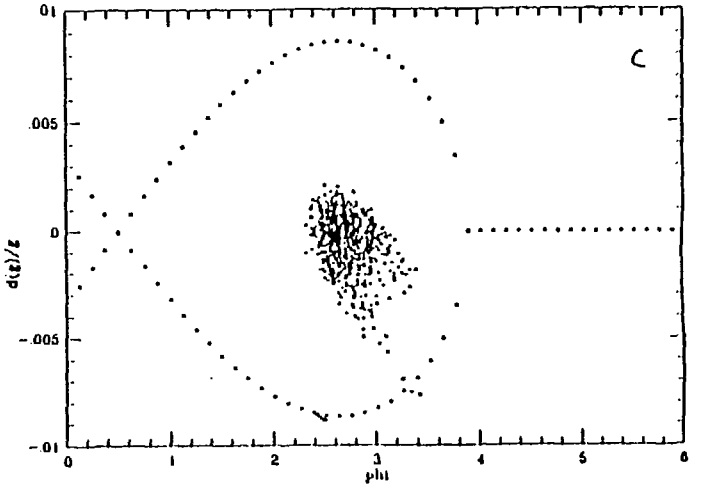

+80 ms

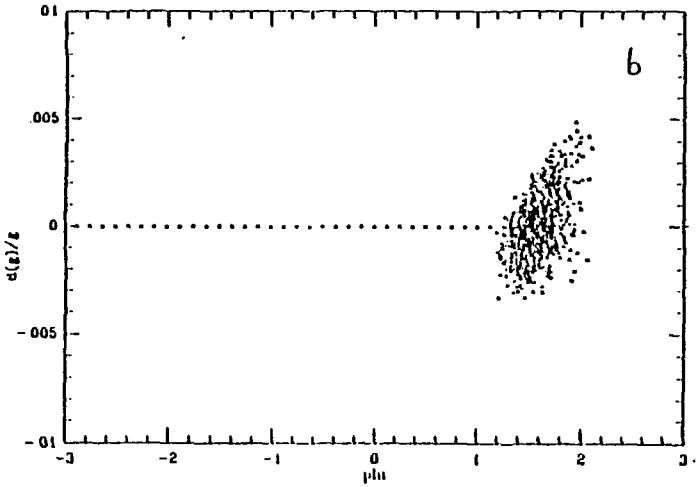

0 ms

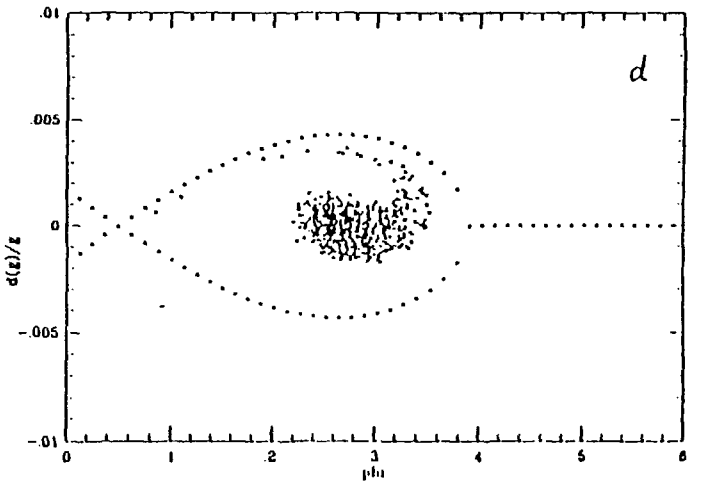

+320 ms

Fig. 2

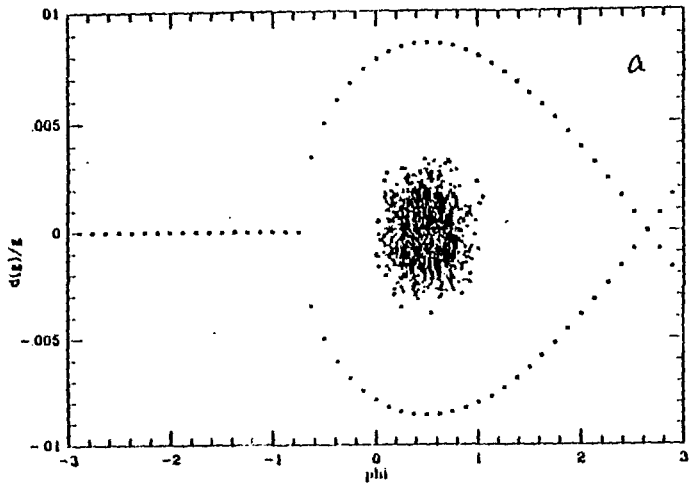

−80 ms

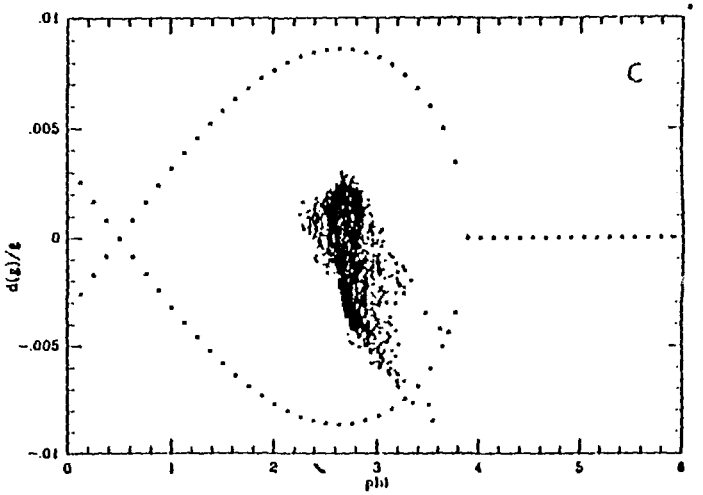

+80 ms

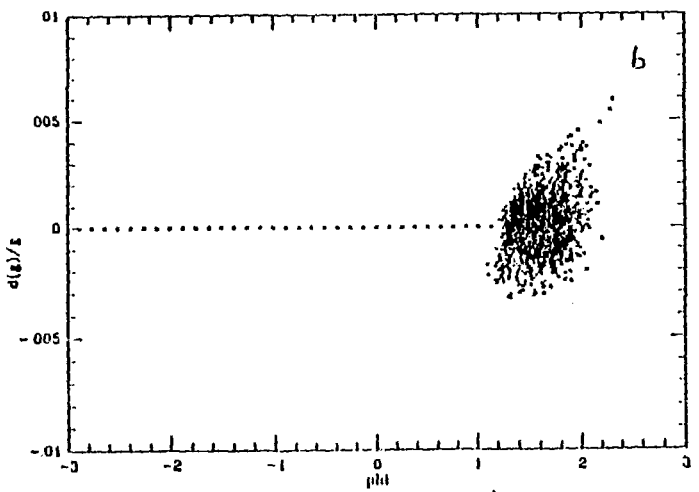

0 ms

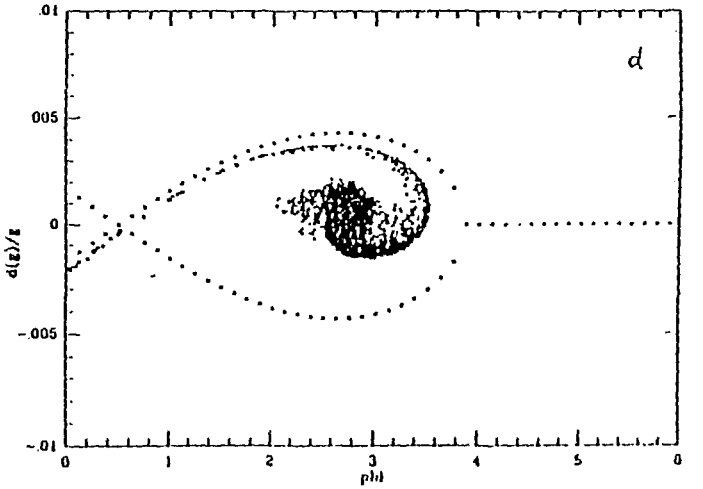

+320 ms

Fig. 3

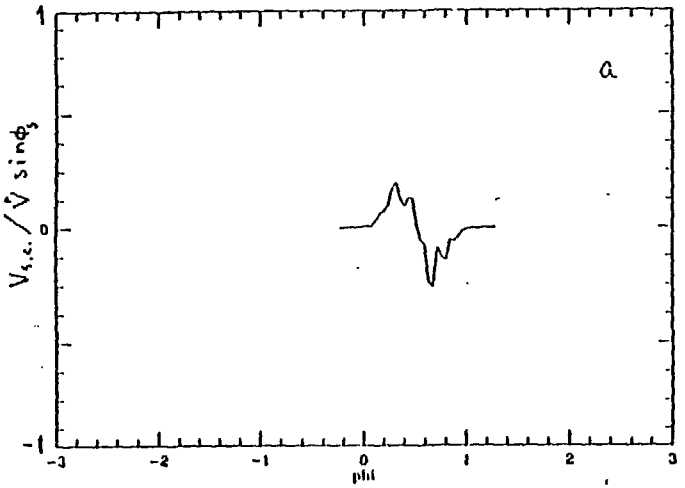

-80 ms

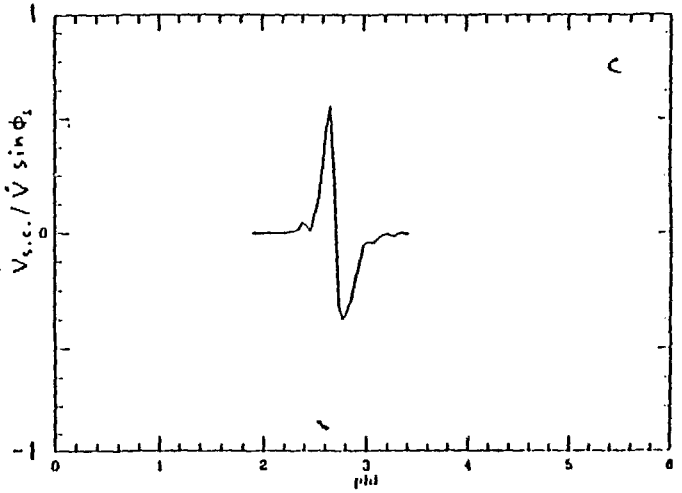

+80 ms

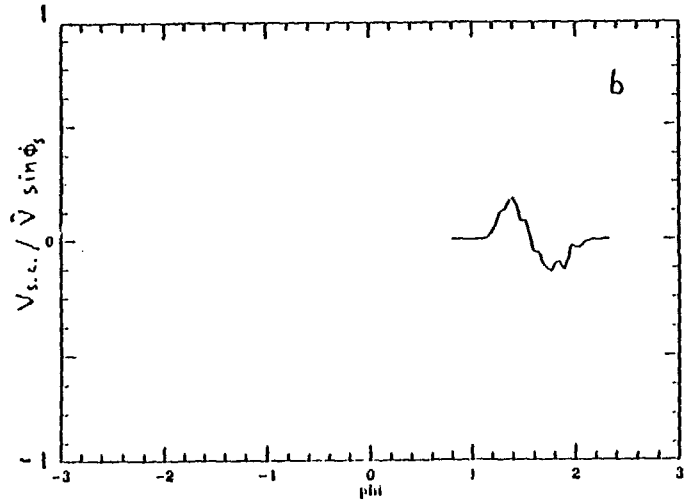

0 ms

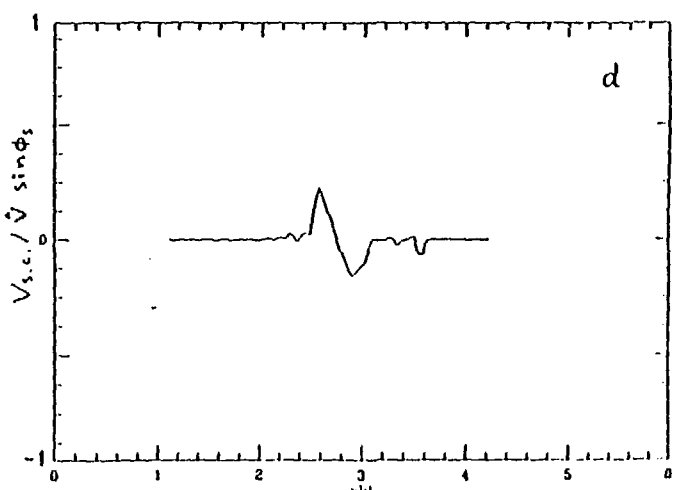

+320 ms

Fig. 4

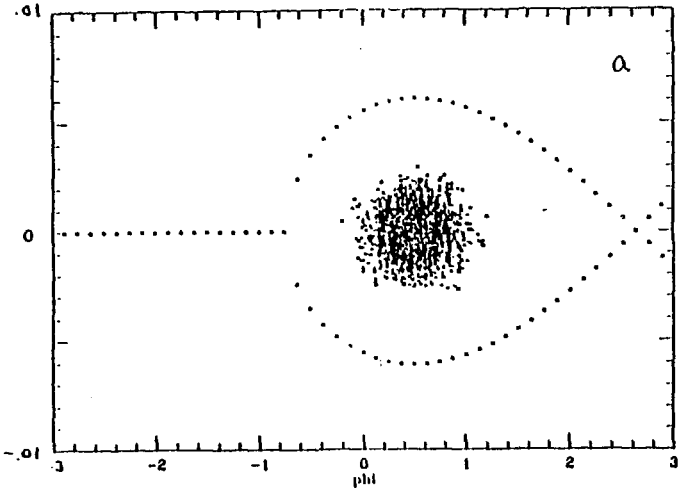

−160 ms

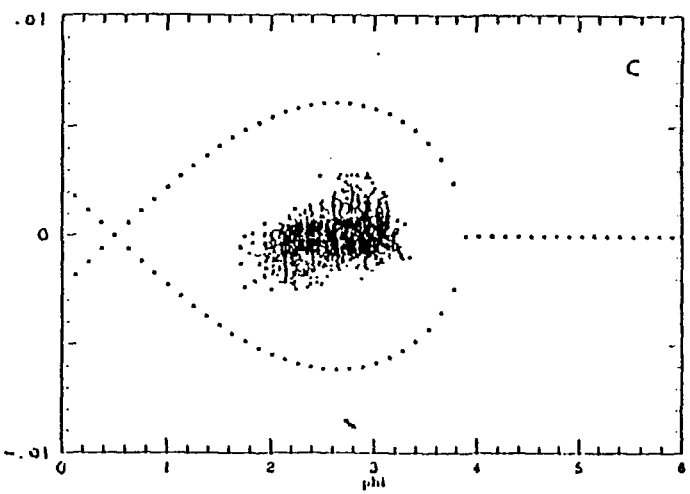

+160 ms

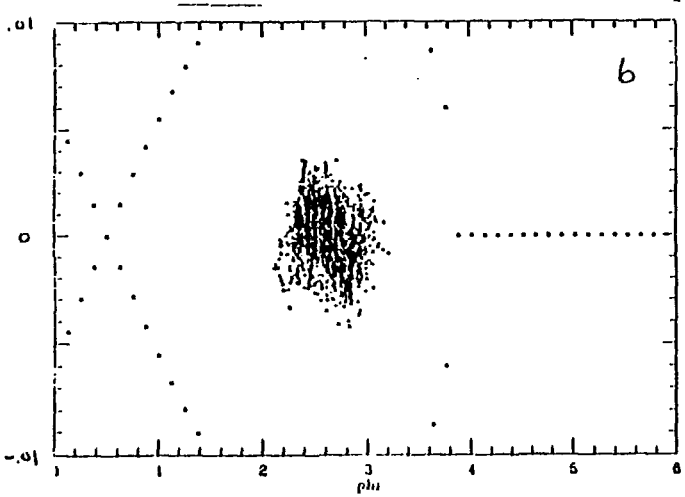

+25 ms

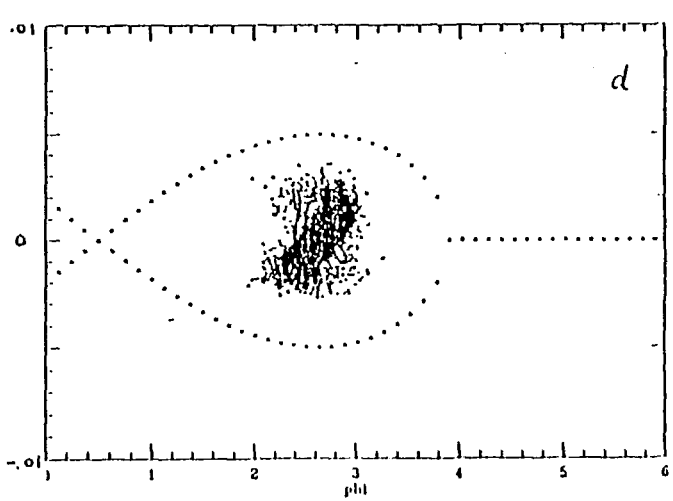

+240 ms

Fig. 5

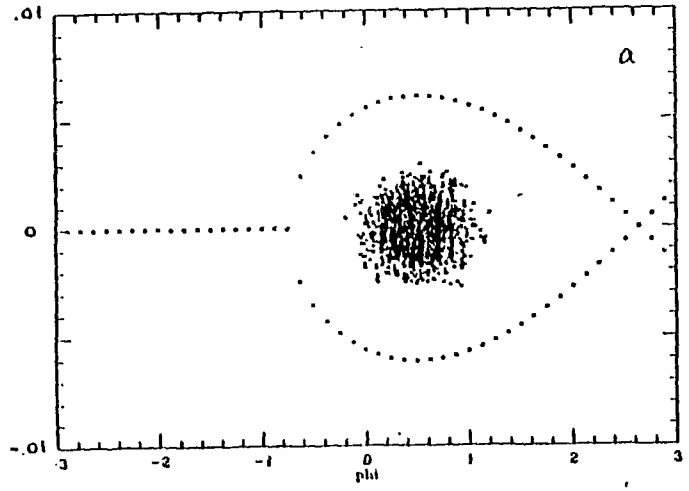

-160 ms

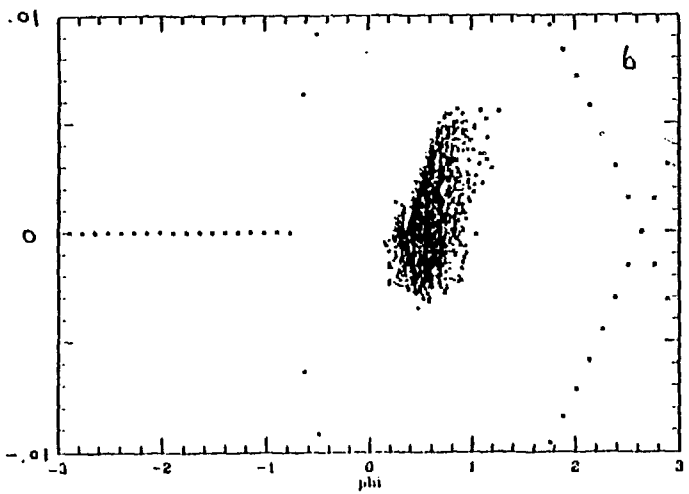

-25 ms

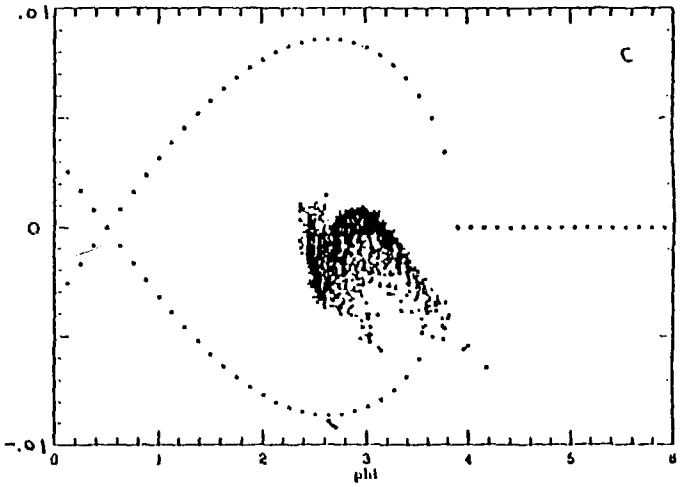

+80 ms

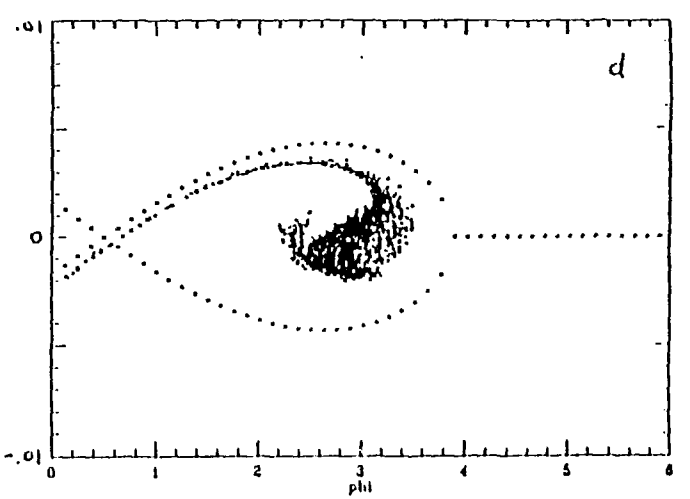

+320 ms

Fig. 6

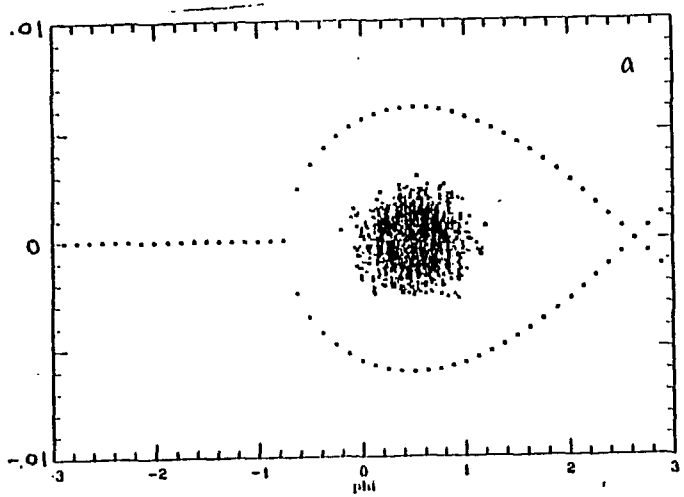

-160 ms

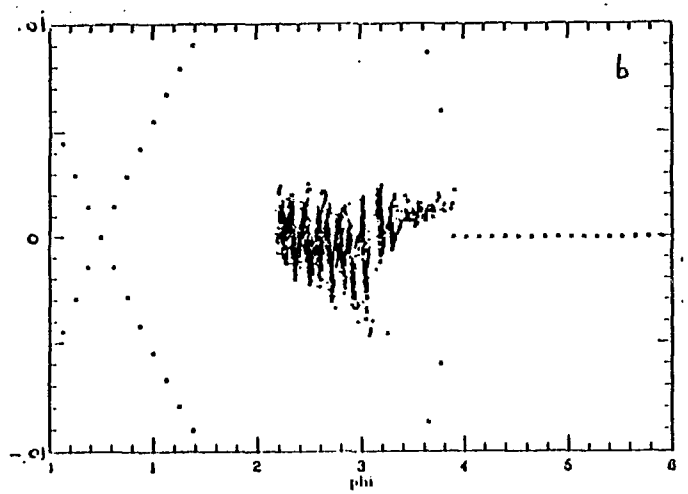

+25 ms

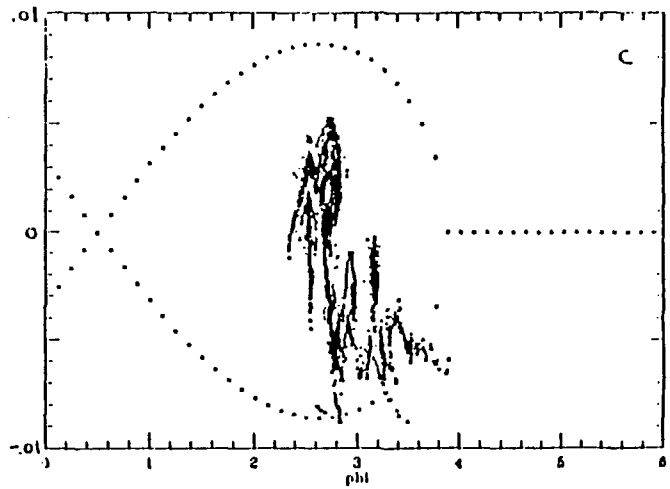

+80 ms

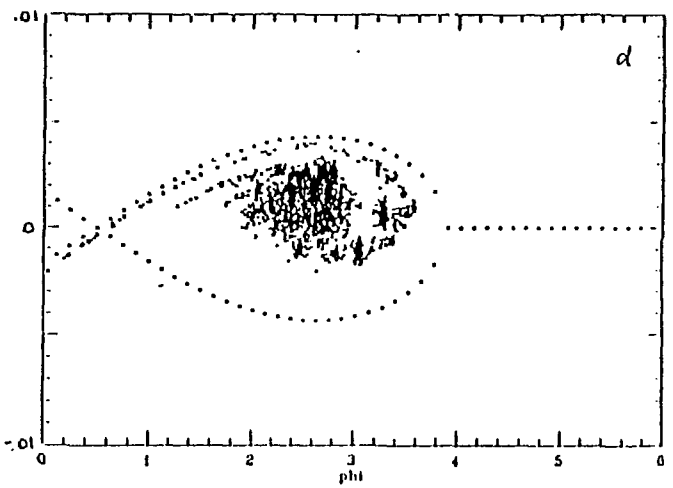

+320 ms

Fig. 7

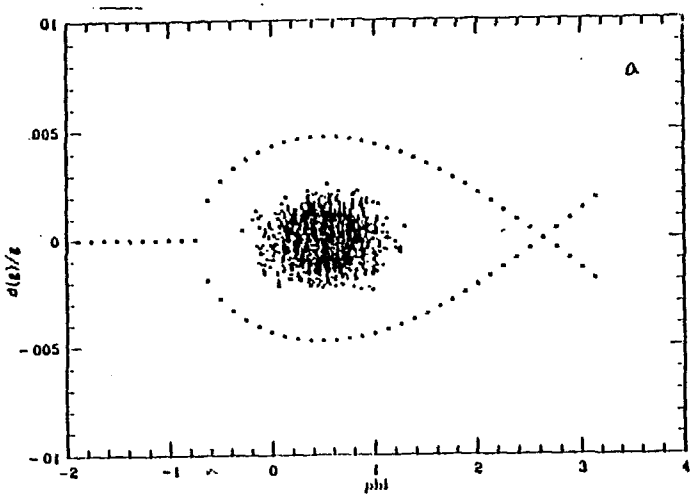

-80 ms

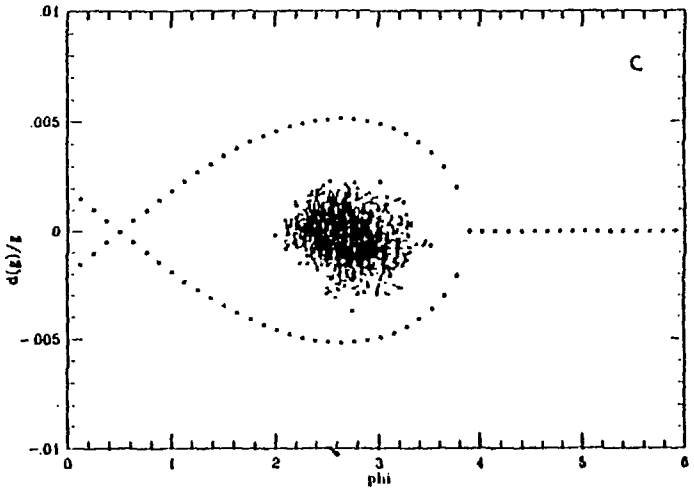

+25 ms

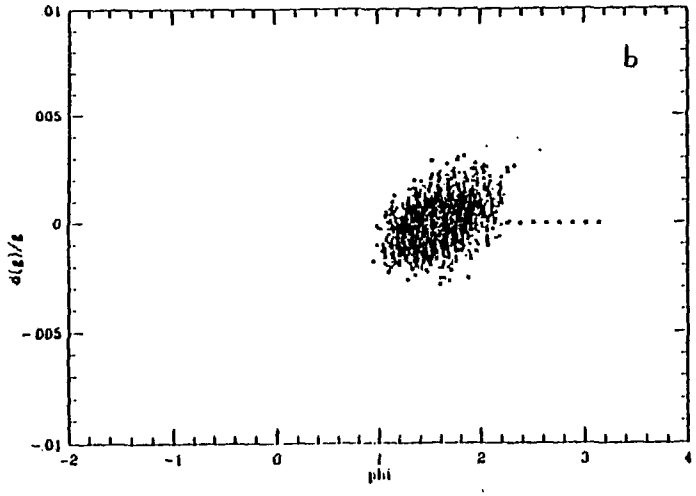

0 ms

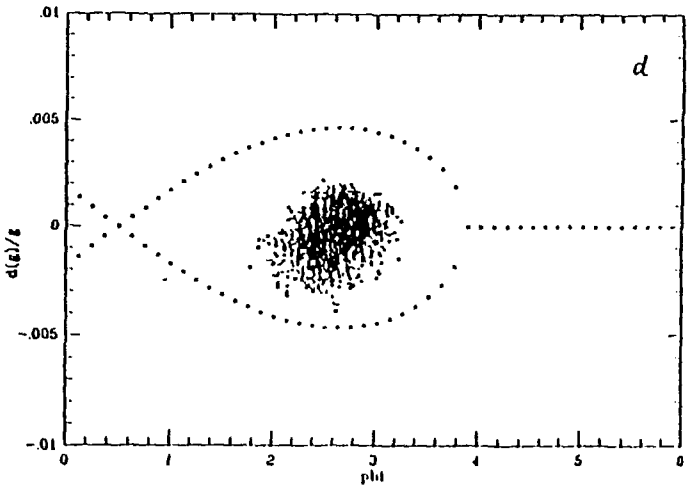

+80 ms

Fig. 8

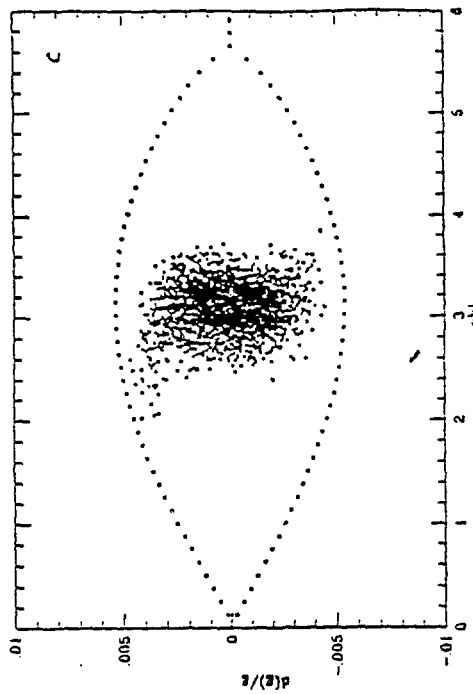

58 ms

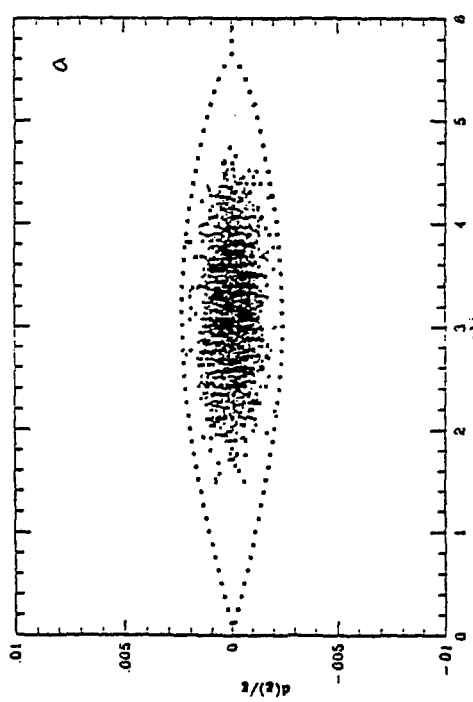

0 ms

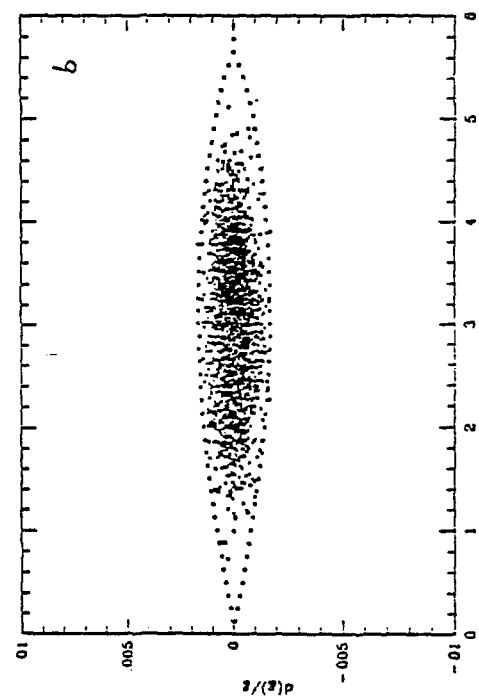

50 ms

Fig. 9

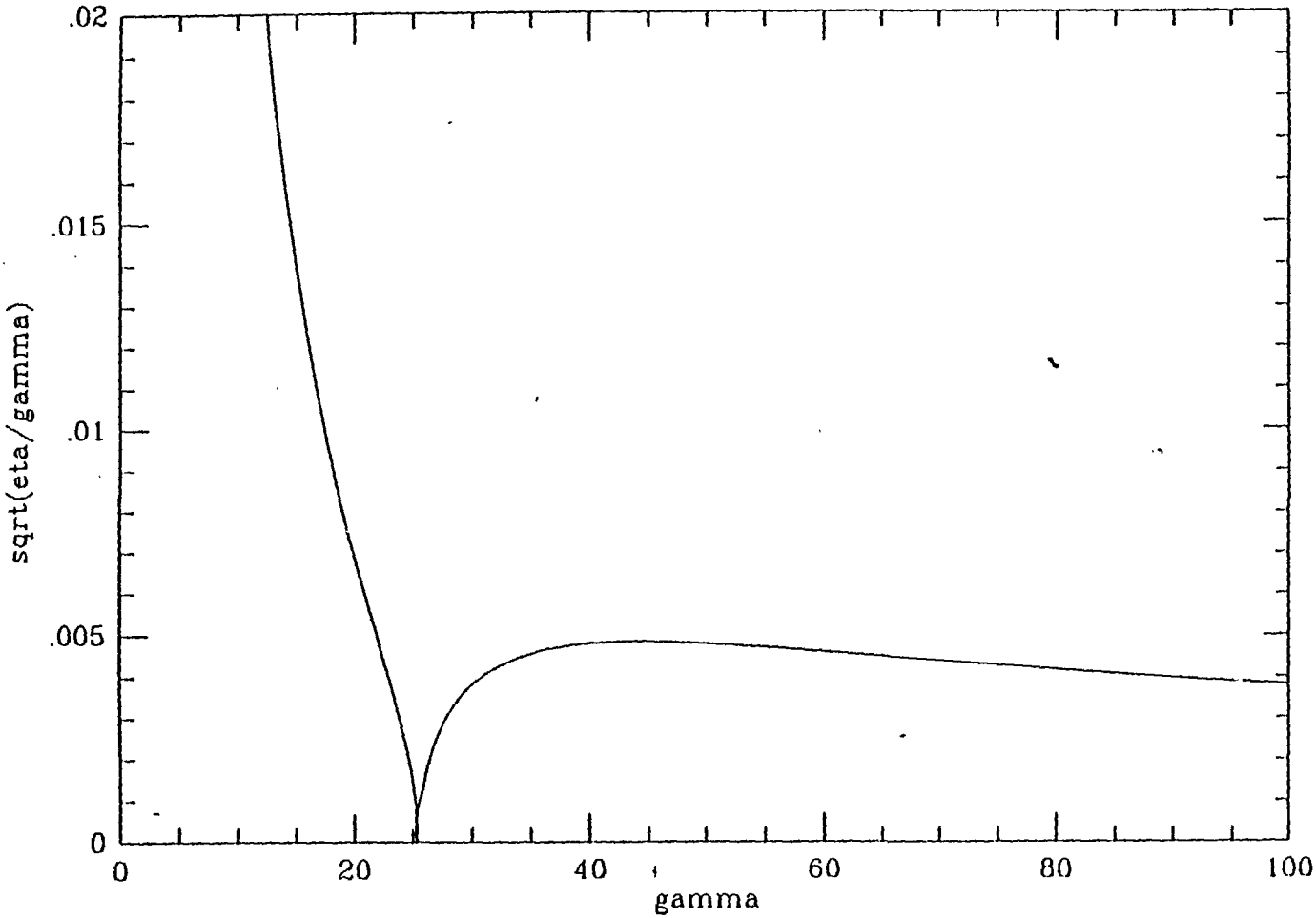

Fig. 10

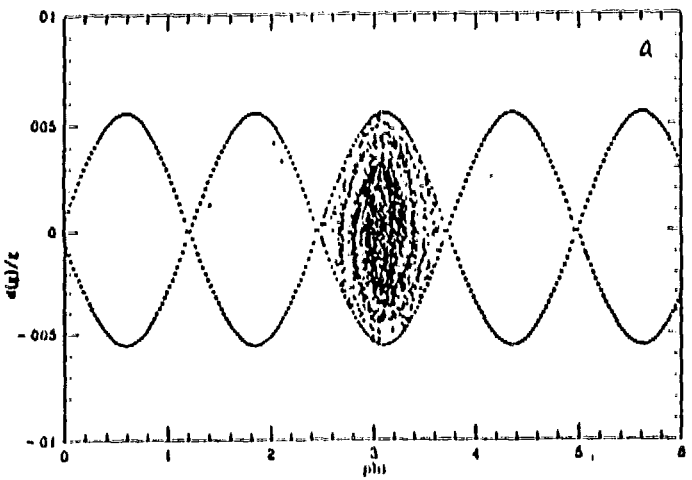
a
0.1
0.05
0
-0.05
-0.1
0
1
2
3
4
5
6
phi

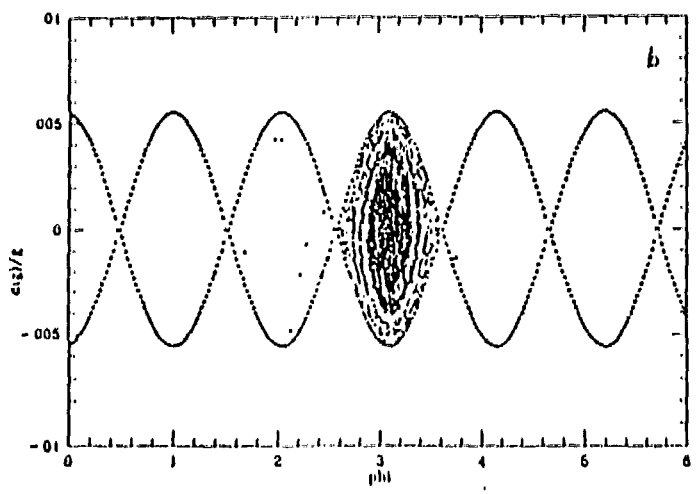
b
0.1
0.05
0
-0.05
-0.1
0
1
2
3
4
5
6
phi

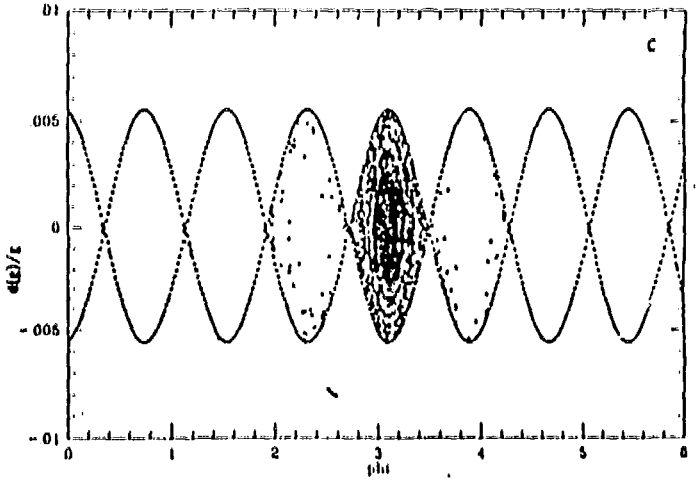
c
0.1
0.05
0
-0.05
-0.1
0
1
2
3
4
5
6
phi

Fig. 11

330

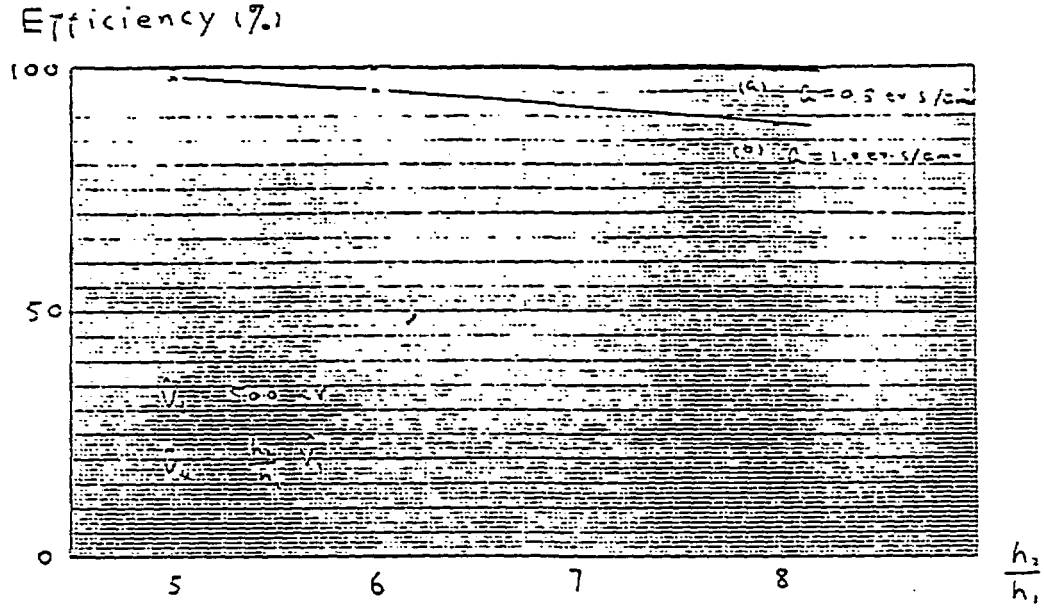
Efficiency (%)
100
50
0
5
6
7
8
$\frac{h_2}{h_1}$

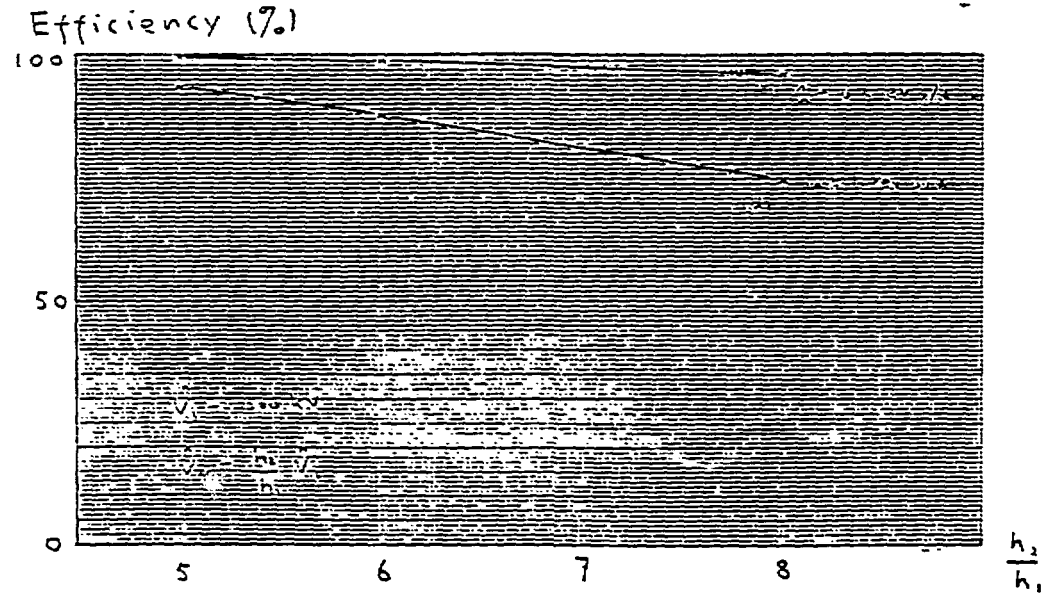
Efficiency (%)
100
50
0
5
6
7
8
$\frac{h_2}{h_1}$

Fig. 12

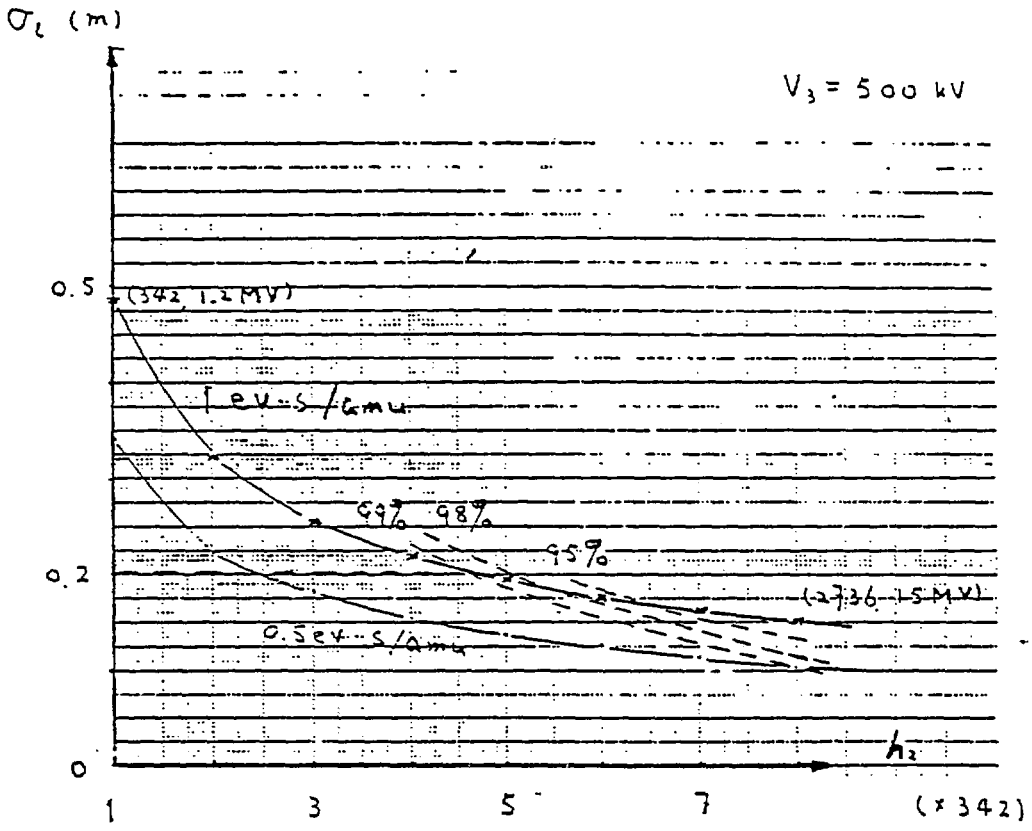
σ_l (m)
V_3 = 500 kV
0.5
(342 1.2MV)
1 ev-s/amu
99% 98%
95%
0.2
(2736 1.5MV)
0.3ev-s/amu
0
h_2
1
3
5
7
(×342)

Fig. 13

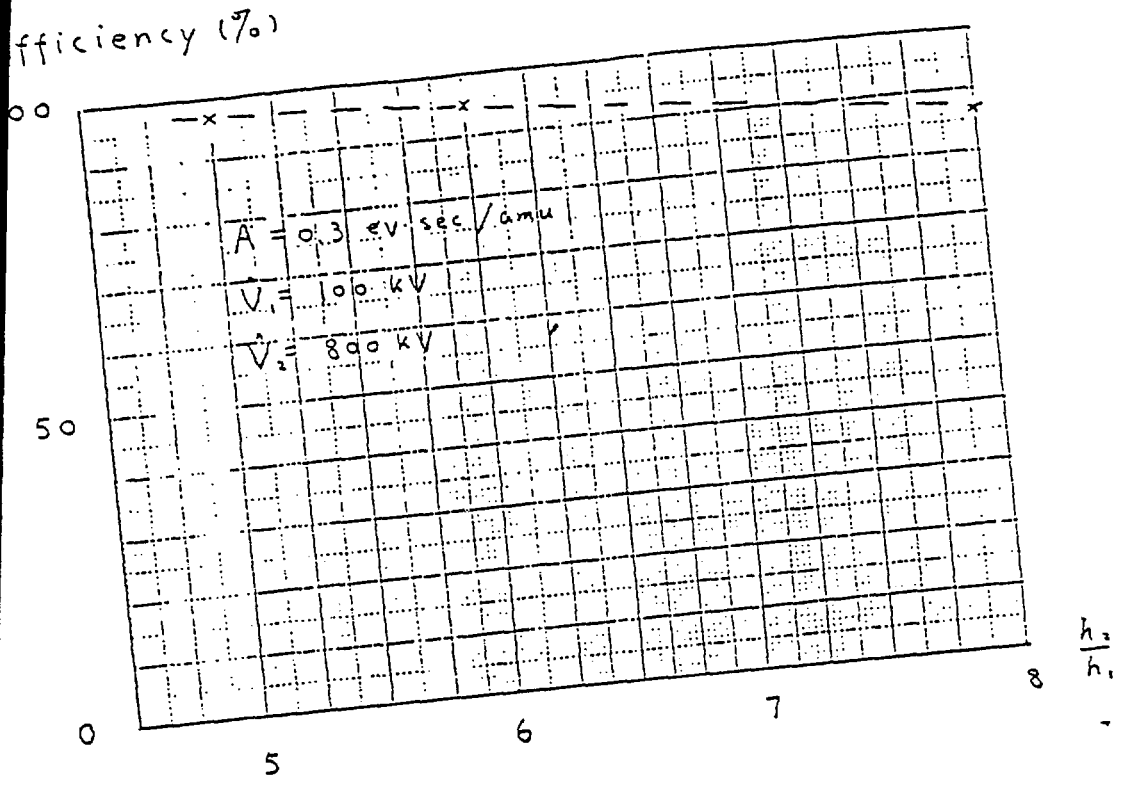

Fig. 14